Translational Oncology 13 (2020) 100746

Contents lists available at ScienceDirect

Translational Oncology

journal homepage: www.elsevier.com/locate/tranon

Low Incidence of High-Grade Pancreatic Intraepithelial Neoplasia Lesions in a *Crmp4* Gene–Deficient Mouse Model of Pancreatic Cancer

Keiichi Yazawa [a,b], Fumio Nakamura [b,c], Daiki Masukawa [b], Sho Sato [a], Yukihiko Hiroshima [a], Yasuhiro Yabushita [a], Ryutaro Mori [a], Ryusei Matsuyama [a], Ikuma Kato [d], Hideki Taniguchi [e], Yoshio Goshima [b,]*, Itaru Endo [a]

[a] *Department of Gastroenterological Surgery, Yokohama City University Graduate School of Medicine, Yokohama, Japan*
[b] *Department of Molecular Pharmacology and Neurobiology, Yokohama City University Graduate School of Medicine, Yokohama, Japan*
[c] *Department of Biochemistry, Tokyo Women's Medical University, School of Medicine, Tokyo, Japan*
[d] *Department of Molecular Pathology, Yokohama City University Graduate School of Medicine, Yokohama, Japan*
[e] *Department of Regenerative Medicine, Yokohama City University Graduate School of Medicine, Yokohama, Japan*

ARTICLE INFO

Article history:
Received 26 September 2019
Received in revised form 30 January 2020
Accepted 30 January 2020
Available online xxxx

ABSTRACT

Pancreatic intraepithelial neoplasia (PanIN), the most common premalignant lesion of the pancreas, is a histologically well-defined precursor to invasive pancreatic ductal adenocarcinoma (PDAC). However, the molecular mechanisms underlying the progression of PanINs have not been fully elucidated. Previously, we demonstrated that the expression of collapsin response mediator protein 4 (CRMP4) in PDAC was associated with poor prognosis. The expression of CRMP4 was also augmented in a pancreatitis mouse model. However, the role of CRMP4 in the progression of PanIN lesions remains uncertain. In the present study, we examined the relationship between CRMP4 expression and progression of PanIN lesions using genetically engineered mouse models. PanIN lesions were induced by peritoneal injection of the cholecystokinin analog caerulein in *LSL-KRAS*^{G12D}*; Pdx1-Cre* (KC-*Crmp4* wild-type, WT) mice and *LSL-KRAS*^{G12D}; *Pdx1-Cre*; *Crmp4*$^{-/-}$ (KC-*Crmp4* knockout, KO) mice. We analyzed pancreatic tissue sections from these mice and evaluated PanIN grade by hematoxylin and eosin staining. CRMP4 expression was examined and the cellular components assessed by immunohistochemistry using antibodies against CRMP4, CD3, and α-smooth muscle actin (SMA). The incidence of high-grade PanIN in KC-*Crmp4* WT mice was higher than that in KC-*Crmp4* KO animals. CRMP4 was expressed not only in epithelial cells but also in αSMA-positive cells in stromal areas of PanIN lesions. The CRMP4 expression in stromal areas correlated with PanIN grade in WT mice. These results suggested that the expression of CRMP4 in stromal cells may underlie the incidence or progression of PanIN.

Introduction

Pancreatic ductal adenocarcinoma (PDAC) constitutes a leading cause of cancer death [1,2], primarily owing to the lack of effective early detection methods and poor efficacy of existing therapies. Moreover, even among the 10% to 20% of patients who received a diagnosis of surgically resectable PDAC, most ultimately die of recurrent and metastatic disease [3]. These low survival rates are attributed in part to the fact that PDAC metastases have often progressed to the point where surgical removal cannot provide a cure. In order to improve the cancer mortality, detection and treatment in the early phase are necessary. Toward this end, analyses of PDAC pathological specimens and of genetically engineered PDAC mouse models have suggested that PDAC develops from pancreatic intraepithelial neoplasia (PanIN) [4,5].

PanIN represents the most common pancreatic precursor lesion. An activating K-*ras* point mutation is almost uniformly present in early stage PanIN, whereas subsequent inactivating mutations in p16, p53, and Smad4 occur in advanced lesions [6–9]. The development of genetically engineered mouse models with PDAC, such as *Pdx1-Cre; LSL-Kras*^{G12D} [10], *Pdx1-Cre; LSL-Kras*^{G12D}*; Ink4a/Arf*$^{flox/flox}$ [11], and *Pdx1-Cre; LSL-Kras*^{G12D}*; LSL-p53*^{R172H} [7], has facilitated our understanding of the molecular mechanisms of pancreatic neoplasia [10,12].

Recently, collapsin response mediator proteins (CRMPs), also known as the dihydropyrimidiase-like protein (DPYSL) family, have been shown to be involved in malignant tumors [13–20]. Altered expression of different CRMPs has been observed in various malignant tumors including lung, breast, colorectal, prostate, liver, gastric, pancreatic, and neuroendocrine lung cancer [21]. CRMPs were originally identified as the intracellular signaling mediators of a repulsive axon guidance molecule, semaphorin-3A (Sema3A) [22]. The CRMP family consists of five members, CRMP1-5 [23,24], which are highly expressed in the developing and adult nervous system. CRMPs are involved in axon guidance, axonal elongation, cell migration, synapse maturation, and the generation of neural polarity

* Address all correspondence to: Yoshiro Goshima, Department of Molecular Pharmacology and Neurobiology, Yokohama City University Graduate School of Medicine, 3-9 Fukuura, Kanazawa-ku, Yokohama, 236-0004, Japan.
E-mail address: goshima@med.yokohama-cu.ac. (Y. Goshima).

http://dx.doi.org/10.1016/j.tranon.2020.100746

[22,25,26]. In these developmental processes, CRMPs play critical role in regulating cytoskeletal rearrangement, which is largely mediated by their phosphorylation-dependent interaction with F-actin and microtubules [27,28]. CRMPs can be phosphorylated by various kinases including Cdk5, GSK3β, Rho-kinase, and Fyn [29–34]. In addition, CRMPs have also been implicated in a variety of cellular and molecular events such as inflammation and cell growth in peripheral tissues or organs as well as in the central nervous system [35–37].

Similar to other CRMP family proteins, CRMP4 is highly expressed in the central nervous system. CRMP4 expression is also observed in malignant tumors originated from various organs including the intestine, liver, pancreas, and prostate [14,38–45]. However, the roles of CRMP4 in tumorigenesis or tumor progression remain unknown. Overexpression of CRMP4 suppresses the invasion ability and inhibits tumor metastasis of prostate cancer cells [14]. Consistent with this, lower expression of *CRMP4* mRNA in hepatocellular carcinoma tissues is associated with shorter recurrence-free survival and subsequent adverse prognosis [42]. In contrast, high expression levels of *CRMP4* mRNA in gastric cancers are significantly associated with shortened recurrence-free survival [39]. Previously, we reported that CRMP4 expression is associated with poor prognosis through the promotion of liver metastasis of pancreatic cancer [43]. In addition, CRMP4 knockdown using siRNA reduces the cellular invasion of Capan-1 cells, a human pancreas adenocarcinoma cell line. CRMP4 expression was also found to be enhanced in the pancreatic parenchyma and the infiltrated lymphocytes in pancreatic tissue of a pancreatitis mouse model [46]. In turn, a meta-analysis of chronic pancreatitis has shown a relative risk of 13.3 for developing malignancy [47], and chronic pancreatitis is considered to have a strong relationship with carcinogenesis and pancreatic cancer [48]. Together, these findings suggest that CRMP4 is involved in the pathogenesis of pancreatic cancer, although direct causality has not been demonstrated. To further clarify the role of CRMP4 in in pancreatic carcinogenesis, in this study, we examined the role of CRMP4 in the progression of PanIN in a genetically engineered mouse model of pancreatic cancer.

Materials and Methods

Ethics Statement

All animal procedures were performed according to the Guide for the Care and Use of Laboratory Animals (Japanese Association for the Laboratory Animal Science) and the Guide for Yokohama City University. Specific approval for the mouse experiments was obtained from the Institutional Animal Care and Use Committee of Yokohama City University School of Medicine with the protocols F-A-15-042 and F-A-16-019 "Biological function of CRMP4 in metastasis and invasion with pancreatic cancer model mice." All surgical procedures were performed under isoflurane (Pfizer, New York, NY) and pentobarbital sodium (Kyoritsu seiyaku, Tokyo, Japan) anesthesia, and all efforts were made to minimize the number of animals used and their suffering.

Reagents

Antibodies purchased were as follows: polyclonal rabbit anti-CRMP4 (AB5454, Merck Millipore, Darmstadt, Hessen, Germany), monoclonal rabbit anti-CD3 (ab5690, Abcam, Cambridge, Cambridgeshire, UK), and monoclonal mouse anti–α-smooth muscle actin (SMA) (14-9760, eBioscience, San Diego, CA). Alexa Fluor 488 Goat Anti-rabbit-IgG and Alexa Fluor 594 Goat Anti-mouse-IgG antibodies were purchased from Life Technologies (Carlsbad, CA).

Purification of Recombinant CRMP4 Peptide

GST-fused CRMP4 fragment was expressed in *Escherichia coli* BL21 strain [35], and CRMP4 was affinity-purified using glutathione-resin following digestion with Prescission protease (GE Healthcare, Little Chalfont, Buckinghamshire, UK) [35].

Animals

Wild-type (WT) C57BL/6JJmsSLc male mice were purchased from Japan SLC (Hamamatsu, Shizuoka, Japan). All mice were maintained at the animal care facility of Yokohama City University under a 12-hour light/12-hour dark cycle at 23°C ± 1°C, with free access to water and food. All mice were fed commercially available MF feed (Oriental Yeast Kogyo Co., Tokyo, Japan).

We used a genetic strategy to selectively knock-in the *K-ras* mutation in the pancreas. Using the Cre/loxP system, we crossed *LSL-KRAS*^{G12D} mice and *Pdx1-Cre* mice to generate *LSL-KRAS*^{G12D}*; Pdx1-Cre* (KC-*Crmp4* WT) mice, which exhibit conditional *K-ras* mutation in the pancreas [10,49]. *Crmp4*$^{-/-}$ mice were established as previously described (Acc. No. CDB0637K) and maintained on a 129/SV X C57BL/6J hybrid background [50–52].

The *Pdx1-Cre* transgenic mouse strain, *LSL-KRAS*^{G12D} knock-in mouse strain, and *Crmp4*$^{-/-}$ mouse strain were intercrossed. *LSL-KRAS*^{G12D} knock-in and *Crmp4*$^{-/-}$ mice were interbred to generate *Pdx1-Cre*; *LSL-Kras*^{G12D}; *Crmp4*$^{-/-}$ (KC-*Crmp4* KO) mice (Figure 1, *A* and *B*).

Genotyping of Animals

Genotyping of the *CRMP4* allele was performed by polymerase chain reaction (PCR) using the following primers: *Crmp4* fourth intron Rv, 5′-CAC TGG CCT GGC TGA AGA TCA A-3′; *Crmp4* WT Fw, 5′-GTC AAG CTG CTA AAG GAG CCT-3′; and CDB-Neo Fw, 5′-GGC GAG GAT CTC GTC GTG ACC-3′. The PCR was performed with 30 cycles of 95°C for 30 seconds, 62°C for 30 seconds, and 72°C for 1 minute to obtain a 790-bp mutant allele and a 427-bp WT allele.

Genotyping of the *LSL-Kras*^{G12D} allele was performed by PCR using the following primers: *Kras* Y116-common, 5′-TCC GAA TTC AGT GAC TAC AGA TG-3′; *Kras* Y117-LSL, 5′-CTA GCC ACC ATG GCT TGA GT-3′; and *Kras* Y118-wt, 5′-ATG TCT TTC CCC AGC ACA GT-3′. The PCR was performed with 35 cycles of 95°C for 30 seconds, 60° C for 30 seconds, and 72°C for 30 seconds. The expected product size of Y117/Y116 is 327 bp for LSL, and that of Y116/Y118 is 450 bp for WT. Genotyping of the Pdx1-Cre allele was performed by PCR using the following primers: Pdx1-Cre Rv, 5′-GGT GTA CGG TCA GTA AAT TTG-3′ and Pdx1-Cre Fw, 5′-CTG GAC TAC ATC TTG AGT TGC-3′. The PCR was performed with 35 cycles of 95°C for 30 seconds, 60°C for 30 seconds, and 72°C for 30 seconds to obtain a 650-bp product size.

Acute Pancreatitis-Induced PanIN Lesions in Conditional K-ras Mutant Mice

In order to investigate the role of CRMP4 in PanIN development, acute pancreatitis was induced in KC mice [53] by treatment with the cholecystokinin analog caerulein (C9026, Sigma-Aldrich, St. Louis, MO) [54]. Working aliquots (1 ml) at 100 μg/ml were stored at −20°C until use, at which time it was dissolved in phosphate buffered saline (PBS), pH 7.4, at a concentration of 10 μg/ml. Acute pancreatitis was induced by seven hourly intraperitoneal injections of caerulein (50 μg/kg) at the age of 7-10 weeks, which were repeated 48 hours later [53]. PanIN lesions developed with 3-4 months. The pancreas was removed at day 73-216 from the last injection. We also examined PanIN formation in the *Crmp4*$^{-/-}$ background. Caerulein was administered to *LSL-KRAS*^{G12D}; *Pdx1-Cre*; *Crmp4*$^{-/-}$ (KC-*Crmp4* KO) mice to develop PanIN lesions (Figure 1*C*). Overall, we prepared 30 PanIN model mice (KC-*Crmp4* WT; $n = 19$ and KC-*Crmp4* KO; $n = 11$).

Morphological Analysis of PanIN

Subsequent to euthanasia with an excessive dose of isoflurane and pentobarbital, mice were perfusion-fixed with 4% (wt/vol) paraformaldehyde in PBS. To obtain macroscopic and microscopic findings of both KC-*Crmp4*

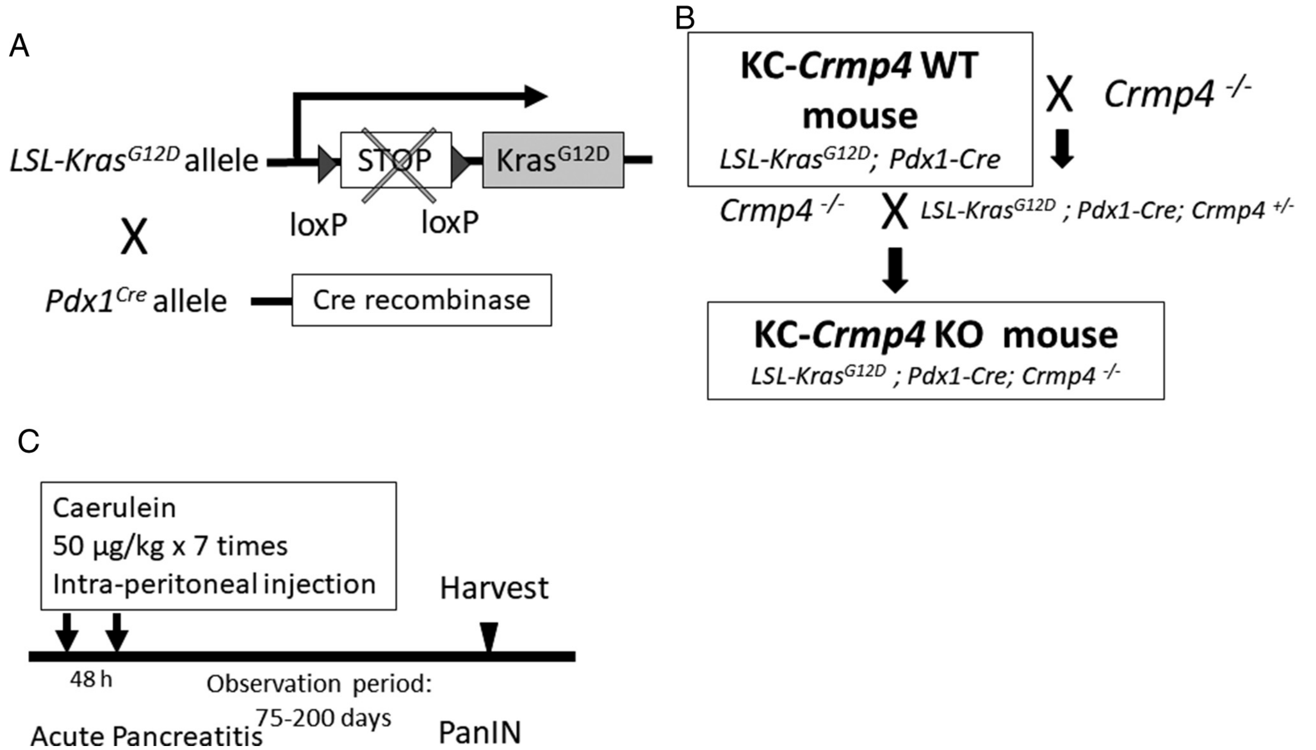

Figure 1. Experimental design. (A) Targeting endogenous KrasG12D expression to the mouse pancreas. *Pdx1-Cre* allele crossed to *LSL-Kras^{G12D}* allele. (B) Genetic makeup of the KC-*Crmp4* KO mouse. *LSL-KRAS^{G12D}*; *Pdx1-Cre* (KC-*Crmp4* WT) mice were crossed with *Crnp4$^{-/-}$* mice. (C) Treatment protocol for caerulein in *LSL-KRAS^{G12D}; Pdx1-Cre* (KC-*Crmp4* WT) (n = 19) and *LSL-KRAS^{G12D}; Pdx1-Cre; Crmp4$^{-/-}$* (KC-*Crmp4* KO) mice (n = 11).

WT mice and KC-*Crmp4* KO mice, the pancreas was removed together with the spleen and duodenum. Collected pancreases were fixed in 4% paraformaldehyde in PBS for 12 hours at 4°C.

Tissues were embedded in paraffin. Paraffin-embedded pancreas sections (3 µm thick) were deparaffinized in xylene and rehydrated sequentially in ethanol. Slides were washed in deionized water, stained with hematoxylin (131-09665, Wako, Osaka, Japan) and eosin (051-06515, Wako) in 60% ethanol, then dehydrated sequentially in ethanol, cleared with xylenes, and mounted with Entellan new (Merck KGaA, Darmstadt, Hessen, Germany). All slides were analyzed by a pathologist (I.K.) for findings of PanIN development. The pathologist was blinded to the tissue genotype. Each slide was classified as normal acinar/ductal cells; acinar-to-ductal metaplasia; PanIN-1A, -1B, -2, or -3; or PDAC based on the classification consensus [55]. Briefly, PanIN-1 constitutes flat (1A) or papillary (1B) lesions of the columnar epithelium with basally oriented, round nuclei. PanIN-2 represents papillary lesions with nuclear hyperchromasia, crowding, and pseudostratification. PanIN-3 indicates papillary, micropapillary, or cribriform lesions with nuclear pleomorphism, frequent loss of nuclear polarity, and mitoses [56,57]. The tissue samples were evaluated at high optical power (objective, 40) for all PanIN lesions in a randomly selected microscopic field. PanINs grade were presented as incidence of the highest grade of PanINs in the tissue regions examined. The grades of PanINs defined were roughly correlated with the density of PanINs in the tissue regions.

Immunohistochemistry

Paraffin-embedded pancreas sections (3 µm thick) were deparaffinized in xylene and rehydrated sequentially in ethanol. Slides were quenched in 0.3% H_2O_2 in 60% methanol for 30 minutes to block endogenous peroxidase activity. Antigen retrieval was performed in 0.01 M citrate buffer (pH 6.0) for 20 minutes at 120°C in autoclave. After blocking nonspecific proteins with 10% normal goat serum (S-1000, Vector Laboratories, Burlingame, CA) in Tris-buffered saline, 0.1% Tween 20, and 0.00025% NaN3, slides were incubated with primary antibody in 2% normal goat serum at 4°C overnight. The Vector ABC-HRP system kit was employed for signal amplification. The proteins were visualized using 3,3′-diaminobenzidine (ImmPACT DAB; K-6100, Vector Laboratories) staining. Finally, slides were counterstained with hematoxylin, dehydrated sequentially in ethanol, cleared with xylenes, and mounted with Entellan new. The primary antibodies and dilutions were anti-CRMP4, 1:1000; anti-CD3, 1:200; and anti-αSMA, 1:200. Anti-CRMP4 and anti-CD3 antibodies were of rabbit origin, for which 30-minute incubation with polyclonal goat anti-rabbit immunoglobulins [Biotinylated anti-rabbit IgG (H + L); BA-1000, Vector Laboratories] preceded the signal amplification step. Anti-αSMA antibody was of mouse origin, for which 30-minute incubation with polyclonal goat anti-mouse immunoglobulins [Biotin-SP (long spacer) affinity-purified goat anti-mouse IgG (H + L); #115-065-146, Jackson Immuno Research Inc., West Baltimore, MD] was utilized. To verify the specificity of the antibody, immunohistochemistry was performed using an anti-CRMP4 antibody (1:1000) preincubated with antigen peptide at 4°C overnight.

For immunohistological evaluation of CRMP4, two investigators, I. K. and K. Y., independently assessed the stained sections. These investigators were blinded to the sources of sections. The intensity of cytoplasmic CRMP4 immunoreactivity was scored as follows: 0, no staining; 1, mild; 2, moderate; and 3, strong. In statistical analyses, scores 0 and 1 were defined as CRMP4 negative, whereas 2 and 3 were defined as CRMP4 positive. For measurement of colocalization between CRMP4, and αSMA or CD3, we quantitated the number of CRMP4-, αSMA-, and CD3-positive cells using serial sections, respectively (n = 3).

Immunofluorescence Staining

The sections were incubated with primary antibody in 2% NGST at 4°C overnight, followed by incubation with Alexa Fluor–conjugated secondary antibodies. Primary antibodies used were polyclonal anti-CRMP4 (1:1000) and monoclonal anti-αSMA (1:500). The samples were counterstained with

DAPI (340-07971, Wako, Osaka, Japan), and examined and photographed with confocal microscope (Fluo View FV1000, Olympus, Tokyo, Japan).

Immunoblot Analysis

After euthanization, the brains were immediately removed from *Crmp4*$^{+/-}$ and *Crmp4*$^{-/-}$ mice and homogenized in immunoprecipitation buffer: 20 mM Tris-HCl (pH 8.0), 150 mM NaCl, 5 mM EDTA, 1 mM NaF, 0.5 mM Na_3VO_4, 1% Triton X-100, and 2% Protease Inhibitor Cocktail (P8340; Sigma-Aldrich). The lysates were centrifuged at 20,400*g* for 5 minutes at 4°C, and supernatants were normalized for total protein concentration. Equal amounts of total protein were separated by 8% sodium dodecyl sulfate–polyacrylamide gel electrophoresis and transferred to a nylon membrane using Ez Fastblot (#2332590, ATTO, Tokyo, Japan). After being blocked with TTBS buffer (25 mM Tris HCl pH 7.4, 137 mM NaCl, 2.7 mM KCl, and 0.2% Tween-20) supplemented with 5% skim milk, the membrane was incubated with primary antibody: anti-CRMP4 antibody (1:2000) diluted in 10% bovine serum albumin at 37°C for 30 minutes. Following 2% skim milk wash, the membrane was incubated with secondary antibody in signal enhancer HIKARI Solution B (#02267-41, Nacalai Tesque, Kyoto, Japan) at 37°C for 30 minutes. After reaction with Lumina Forte (AWBLUF0500, Millipore Merck KGa), an ImageQuant 400 (GE Healthcare) was used to detect the signals.

Statistical Analyses

Data are presented as the means ± standard deviation and were analyzed with the built-in Student's *t* test using SPSS computer software package version 26.0 for Windows (SPSS Inc., Chicago, IL). *P* values of $<.05$ were considered significant. The relationship between the progression of PanIN grade and the expression of CRMP4 was analyzed using Fisher's exact test in R software for Windows version 3.3.2 (R Foundation for Statistical Computing, Vienna, Austria). In all cases, a group size was chosen that produced statistically unambiguous results.

Results

Low-Grade PanIN Progression in KC-Crmp4 KO Compared to KC-Crmp4 WT Mice

Gross pathological findings included swelled pancreas with hard nodular lesions in KC-*Crmp4* WT and KC-*Crmp4* KO mice. No obvious difference was observed between WT and KO mice (Figure 2, *A* and *B*). Histological examination revealed pathological lesions in the pancreatic tissues of WT and KO mice that were similar to those in human PanIN (Figure 2, *C* and *D*). Notably, PanIN-2 lesions were mainly observed in KC-*Crmp4* WT mice (Figure 2*C*, Table 1), which showed a papillary structure with pseudostratification and enlarged nuclei. Conversely, PanIN-1 lesions were mainly observed in KC-*Crmp4* KO mice (Figure 2*D*, Table 1), which consisted of tall columnar cells with basally located nuclei and abundant supranuclear mucin.

Table 1 shows the grade of PanIN in both genotypes. High-grade PanIN lesions (PanIN-2 and -3) were observed more frequently in KC-*Crmp4* WT mice than in KC-*Crmp4* KO mice (Table 1). The acinar-to-ductal metaplasia was similarly observed in both groups. The observation period was 139.2 ± 41.2 days for KC-*Crmp4* WT and 126.0 ± 23.1 days for KC-*Crmp4* KO mice (Student's *t* test, $P = .340$).

Increased Expression of CRMP4 in PanIN Lesions

We first validated the sensitivity and specificity of the anti-CRMP4 antibody. Western blot analysis using brain lysate revealed that the band detected in *Crmp4*$^{+/-}$ samples was absent in *Crmp4*$^{-/-}$ (Figure 3*A*). In immunohistochemistry using pancreatic tissues, CRMP4 expression was detected in the ductal and acinar cells in *Crmp4*$^{+/+}$ but not in *Crmp4* KO

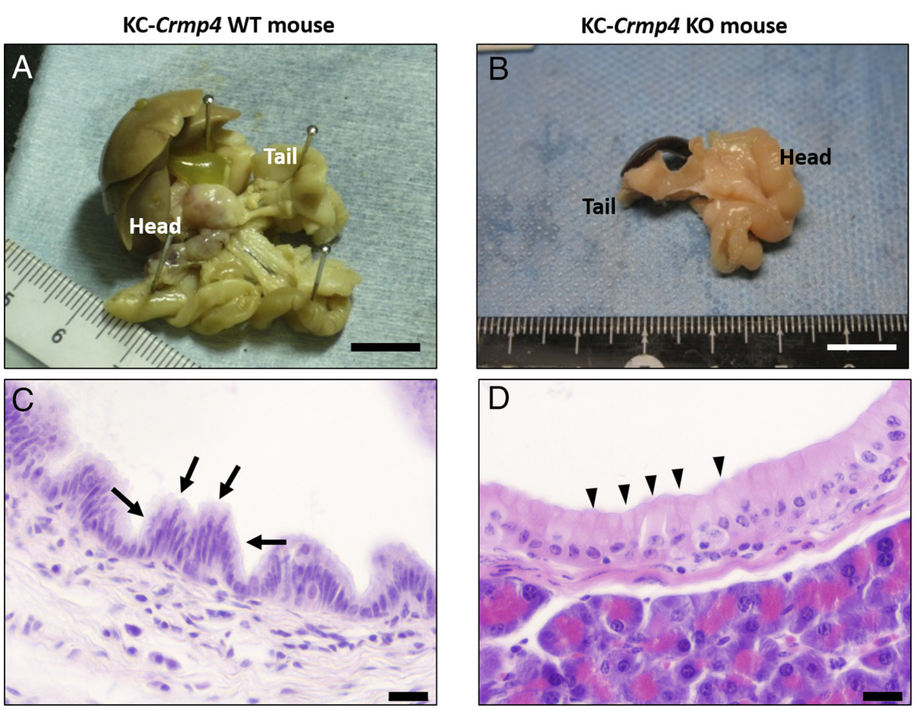

Figure 2. High-grade PanIN lesions in KC-*Crmp4* WT mice. (A, C) Representative findings of PanIN lesions developed in KC-*Crmp4* WT mice. (A) Gross appearance of PanIN-2 lesions. Scale bar, 1 cm. (C) Prominent papillary architecture and mild-to-moderate cytologic atypia including hyperchromasia, increased nuclear size, crowding, pseudostratification, and some loss of polarity are observed. The arrows indicate the representative feature of PanIN-2. Scale bar, 20 μm. (B, D) Representative PanIN lesions in KC-*Crmp4* KO mice. (B) Gross appearance of PanIN-1 lesions. (D) Flat epithelial lesions consisting of tall columnar cells with basally located nuclei and abundant supranuclear mucin are observed. The arrowheads indicate representative feature of PanIN-1. Scale bar, 20 μm. KC-*Crmp4* WT: *LSL-Kras*^{G12D}*; Pdx1-Cre; Crmp4* $^{+/+}$, KC-*Crmp4* KO: *LSL-Kras*^{G12D}*; Pdx1-Cre; Crmp4* $^{-/-}$.

Table 1
PanIN Grade in KC-*Crmp4* WT or KC-*Crmp4* KO Mice

	KC-*Crmp4* WT	KC-*Crmp4* KO
Grade of PanIN	(n = 19)	(n = 11)
Normal or 1	5 (26.3%)	7 (63.6%)
2 or 3	14 (73.7%)	4 (36.4%)

Histological analysis of PanIN progression in KC-*Crmp4* KO compared to KC-*Crmp4* WT mice (χ^2 test; P = .044).

tissue (Figure 3, *E-H*). In WT mice, weak expression of CRMP4 was detected in some of the nuclei of the ductal and acinar cells (Figure 3*F*). CRMP4 expression was also detected in the cytoplasm of cells in PanIN lesions (Figure 3, *G* and *H*) and in the stroma surrounding PanIN lesions (Figure 3, *G* and *H*, black arrowheads).

Preabsorption of anti-CRMP4 antibody with antigen peptide reduced the immune signal (data not shown). These findings supported the specificity of the anti-CRMP4 antibody used.

CRMP4-Positive Cells in Stromal Areas Coincide with αSMA-Positive Cells

To examine the immunohistochemical features of the CRMP4-positive cells in the stromal areas, pancreatic tissues were stained with an antibody against αSMA, the most common marker of fibroblasts/myofibroblasts, and against CD3, a general marker of T cells. Serial sections of PanIN-2 lesions were stained using hematoxylin and eosin along with antibodies against CRMP4, CD3, and αSMA. CRMP4-positive spindle-shaped cells were observed in the stromal areas (Figure 4). The staining pattern of CRMP4 was similar to that of αSMA but not of CD3 (Figure 4, *B* and *D*, black arrowheads). Quantitative colocalization analysis was performed. The percentage of colocalization between CRMP4 and αSMA or CRMP4 and CD3 was 39.0% ± 1.95% or 13.7% ± 0.98%, respectively (n = 3, P = .003, Figure 5, *A* and *B*). Immunofluorescence staining of PanIN-2 lesion (Figure 6, *C* and *D*, yellow arrowhead) illustrated strong expression of CRMP4. Moreover, some stromal cells surrounding the PanIN lesions coexpressed CRMP4- and αSMA-positive cells (Figure 6, *F*, *G* and *H*; white arrowhead).

Immunohistochemical Analysis of CRMP4 in PanIN Lesions and Stromal Areas

To examine the relationship between expression of CRMP4 and the PanIN grade, we evaluated CRMP4 expression in the epithelial cells and stromal cells in PanIN lesions in WT mice. The expression levels of CRMP4 in the epithelial cells of PanIN lesions showed no correlation with PanIN development (Table 2, P = .588). In stromal cells, however, high-grade PanINs were observed more frequently in the CRMP4-positive group than in the CRMP4-negative group (Table 2, P = .023). These results indicated that the expression levels of CRMP4 in the stromal cells of PanIN lesions correlated with the progression of high-grade PanIN in the mouse model of pancreatic cancer. PanIN-1 was found in almost every tissue examined, while PanIN-2 or -3 was rarely seen.

Discussion

In this study, we demonstrated that PanIN progression was suppressed in KC-*Crmp4* KO mice compared with KC-*Crmp4* WT mice. CRMP4 expression was increased in both epithelial cells and the stromal areas of PanIN lesions, especially in αSMA-positive cells. These findings suggested that CRMP4 may participate in the development of PanIN. In addition, CRMP4 expression was observed in in the epithelium of PanIN lesions as well as in normal acinar and ductal cells. This expression profile of CRMP4 in the pancreatic tissue of mice coincides with that in human surgical specimens of PDAC [43]. Whether CRMP4 is also involved in PanIN in human pancreatic cancers thus represents an important issue to be addressed in future studies.

Our study revealed that CRMP4 is expressed in both epithelial cells and in stromal areas, especially in αSMA-positive cells (Figures 4 and 6). Previous studies have shown that the formation of PanIN accompanies the accumulation of a desmoplastic stroma and abundant immune infiltrates [48,58]. It has been suggested that the desmoplastic reaction by inflammation participates in the development of PanIN [59,60]. αSMA-positive cells in stromal areas of PanIN lesions are considered to constitute an active type of pancreatic stellate cells [61]. It is generally accepted that the quiescent type of pancreatic stellate cells, which contain vitamin A, become changed to active type by tissue injury or inflammation [62]. The active type of pancreatic stellate cells accelerates the production of extracellular matrix such

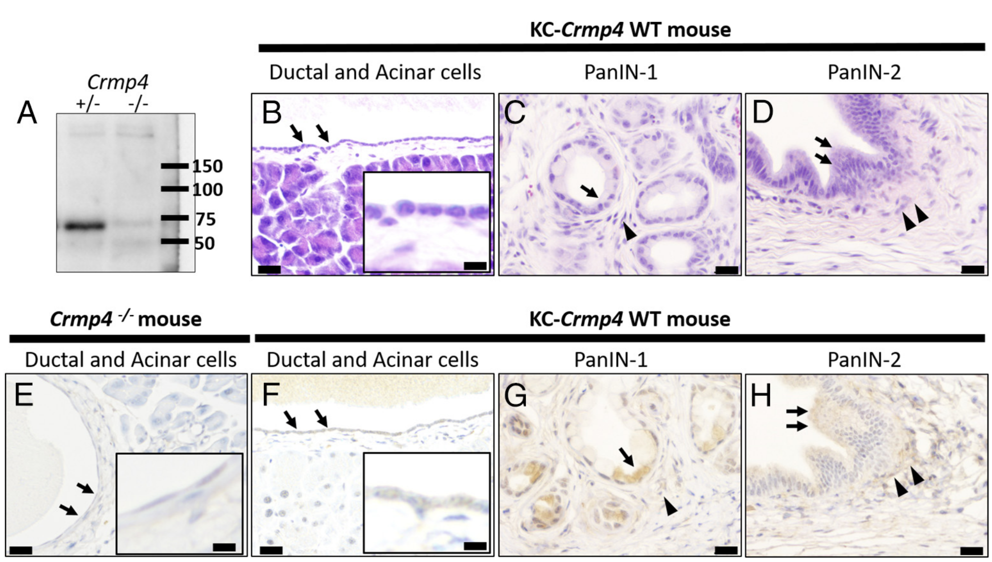

Figure 3. CRMP4 expression in normal pancreatic tissue and in PanIN lesions. (A) Western blot analysis for CRMP4 proteins in brain lysates from *Crmp4*$^{+/-}$ and *Crmp4* KO mice. The band of 66 kDa corresponds to CRMP4, which is missing in brain lysates from *Crmp4* KO mice. Hematoxylin and eosin stain (B-D) and immunostaining with anti-CRMP4 antibody (E-H) in pancreatic tissue. (B, E, F) Representative normal tissue in KC-*Crmp4* WT (B, F) and *Crmp4* KO mice (E). Immunohistochemistry with anti-CRMP4 antibody in KC-*Crmp4* WT (F) and *Crmp4* KO mice (E). (C, G) Representative PanIN-1 in KC-*Crmp4* WT mice. (D, H) Representative PanIN-2 in KC-*Crmp4* WT mice. Expression levels of CRMP4 are relatively high in PanIN lesions (F-H). Arrows indicate PanIN. Arrowheads indicate stromal areas. Scale bar, 20 μm. Insets show higher magnified view of representative areas (B, E, F). Scale bar, 80 μm. The magnification is 1600 times.

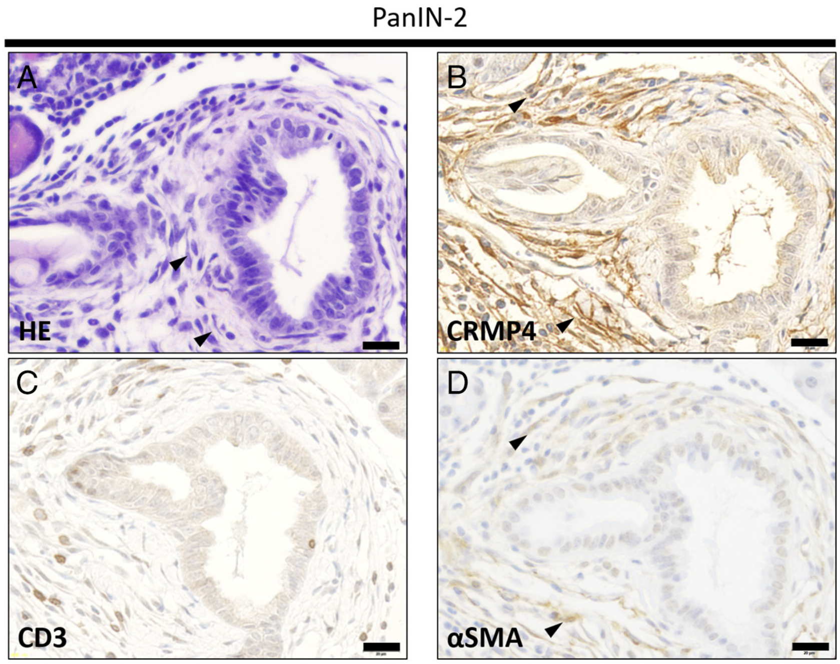

Figure 4. PanIN lesions and stromal areas in pancreatic tissue from KC-*Crmp4* WT mice. (A-D) Serial section of PanIN-2 lesion stained with hematoxylin and eosin (A), anti-CRMP4 (B), anti-CD3 (C), and anti-αSMA antibodies (D). CRMP4-positive cells are coincident with αSMA-positive cells. Scale bar, 20 μm. All sections represent a PanIN-2 lesion in a KC-*Crmp4* WT mouse.

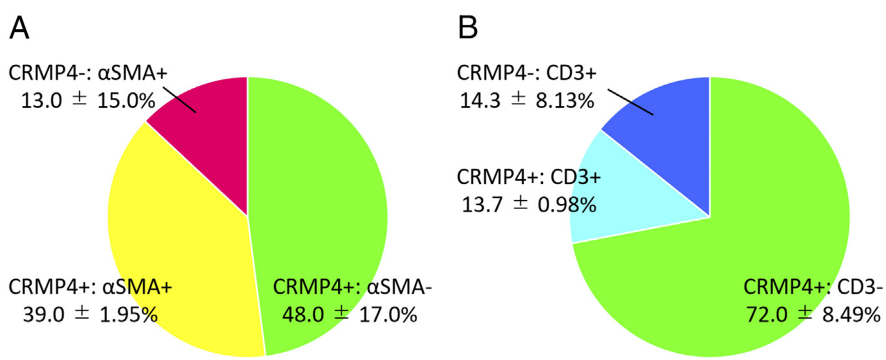

Figure 5. Colocalization of CRMP4 and αSMA or CD3 in stromal areas in KC-*Crmp4* WT mice. (A) The percentages of CRMP4 and αSMA double-positive, CRMP4-positive and αSMA-negative, or CRMP4-negative and αSMA-positive cells in total number of CRMP4 and/or αSMA positive-cells (107.0 ± 46.8/area) were shown. (B) The percentages of CRMP4 and CD3 double-positive, CRMP4-positive and CD3-negative, or CRMP4-negative and CD3-positive cells in total number of CRMP4 and/or CD3 positive-cells (109.7 ± 54.0/area) were shown (n = 3, Student's t test, P = .003).

as collagen, fibronectin, and laminin, thereby leading to pancreas fibrosis [59,63,64]. Therefore, the interaction between pancreatic stellate cells and pancreatic cancer cells or epithelial cells of PanIN may be involved in the proliferation of PDAC or PanIN through the desmoplastic reaction.

Repeated acute pancreatic injury and inflammation serve as contributing factors to the development of pancreatic cancer. In particular, intracellular activation of both pancreatic enzymes and the transcription factor NF-κB comprises an important mechanism that induces acute pancreatitis [65]. Recurrent pancreatic injury owing to genetic susceptibility, along with environmental factors such as smoking, alcohol intake, and conditions such as obesity, leads to increases in oxidative stress, impaired autophagy, and constitutive activation of inflammatory pathways. These processes can stimulate pancreatic stellate cells, thereby increasing fibrosis and encouraging chronic disease development [66]. Fibrosis has a pivotal role in inflammation and carcinogenesis. PDAC is unique among solid tumors because of the extremely dense desmoplastic reaction that surrounds the cancer cell glands of this tumor. The desmoplasia, containing myofibroblastic pancreatic stellate cells, extracellular matrix proteins, and immune cells, modulates the growth of the cancer by providing a scaffold for the cancer cells to grow, along with growth factors, angiogenesis factors, and immune modulators [67]. Considering that activated pancreatic stellate cells underlie the desmoplasia, CRMP4 expression in stellate cells surrounding PanIN lesions may have a critical role in the development of PanIN.

Our previous study demonstrated that CRMP4 was augmented in CD3-positive cells in a pancreatitis mouse model [46]. In comparison, our present study showed that CRMP4-positive cells were coincident with αSMA-positive cells, whereas the expression of CRMP4 was barely detectable in CD3-positive cells. The discrepancy might be attributed to differences in the genetic background of the mouse models, the period of observation, and other experimental conditions. For example, WT and CRMP4 KO mice were examined in acute pancreatitis models [46], whereas WT and CRMP4 KO with K-ras mutant background mice were examined in our current study. It has been shown that K-ras–expressing pancreatic acinar cells initiate microinflammation and that an interaction exists between PanIN and αSMA-positive cells, which may contribute to the formation and progression of PanIN lesions [68]. Furthermore, in our previous study,

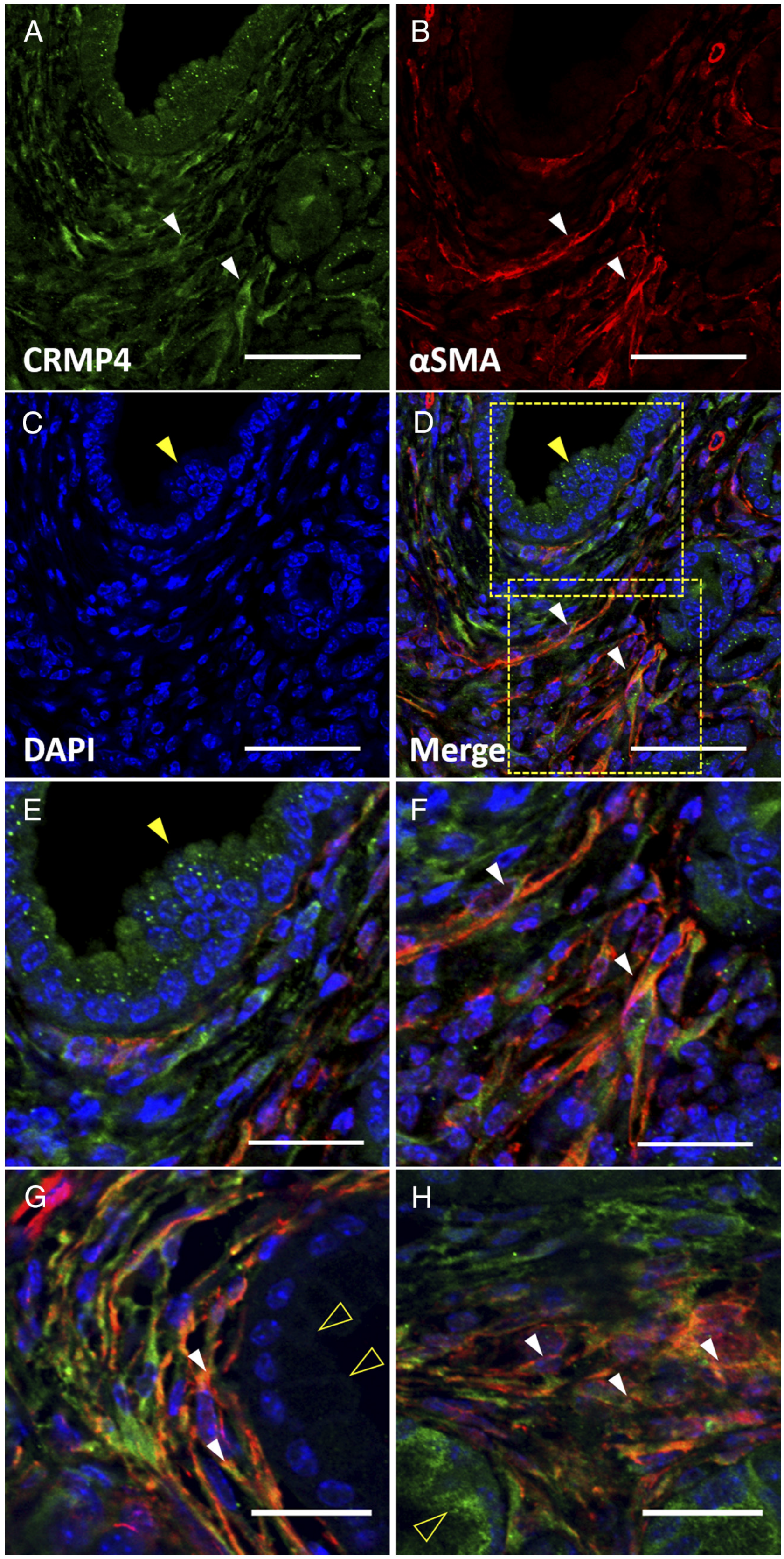

Figure 6. Double immunofluorescence labeling with CRMP4 and αSMA in PanIN-2 lesion in KC-*Crmp4* WT mice. Representative image of PanIN-2 lesion stained with anti-CRMP4 antibody (A), anti-αSMA antibody (B), DAPI (C), and merged image (D). Scale bar, 50 μm. The epithelial cells were CRMP4 positive (yellow arrowhead). Some stromal cells surrounding the PanIN lesions coexpress CRMP4 and αSMA (white arrowhead). Magnified images of boxed areas in the epithelial cells of PanIN lesion and in stromal area in panel D were shown in panels E and F, respectively. Scale bar, 25 μm. The representative CRMP4 and αSMA double-positive cells (white arrowhead) in stromal areas surrounding the PanIN-1A (opened arrowhead) were shown in panels G and H. Scale bar, 25 μm. All sections represent PanIN lesions in a KC-*Crmp4* WT mouse.

Table 2
Positive Correlation Between PanIN Grade and CRMP4 Expression in the Stroma

	CRMP4			
	Epithelial Cells		Stromal Cells	
Grade of PanIN	Negative	Positive	Negative	Positive
1A or 1B	3	1	4	0
2 or 3	7	7	4	10

Relationship between PanIN grade and CRMP4 expression in epithelial cells (Fisher's exact test; two-sided, $P = .588$) and stromal cells (Fisher's exact test; two-sided, $P = .023$).

CRMP4/CD3 double-positive cells were observed mainly in the phase of acute pancreatitis [46], whereas in the present study, CRMP4-positive cells were observed in the recovery phase from acute pancreatitis. It is possible that the number of CD3-positive cells may decrease in recovery phase.

CRMP4 may be involved in PanIN or pancreatic cancer pathogenesis through several mechanisms. First, CRMP4 may promote the inflammation pathway in the development of PanIN. It has been shown that K-*ras* mutation and cell injury mediated by inflammation play important roles in the development of PanIN lesions [53]. Previous studies have demonstrated that CRMP4 is involved in inflammation pathways [46,51]. We reported that both acute pancreatitis and chronic pancreatitis augment CRMP4 expression and its phosphorylation in infiltrated CD3 T-cells [46]. Therefore, CRMP4 may play a pivotal role in pancreatic inflammation. Notably, deletion of CRMP4 in a spinal cord injury mouse model promotes the recovery of locomotion via neuroprotection and limited scar formation because CRMP4 deletion suppresses the activation of microglia or macrophages and reactive astrocytes following injury [51]. Therefore, we speculated that CRMP4 may participate in the development of PanIN through the acceleration of inflammation.

Second, CRMP4 may help to develop PanIN lesions through reconstruction of the cytoskeleton, as this may induce morphologic changes comparable to those observed during PanIN development [69]. In a pancreatitis mouse model, it was found that RAS-related C3 botulium substrate 1 (Rac1), which is an effector molecule of EGFR and K-ras, was necessary for caerulein-induced acinar morphologic changes and filamentous actin redistribution [70,71]. CRMP4 is also known to regulate the actin and microtubule growth cone cytoskeleton in hippocampal neurons [27,28,72]. Moreover, the alternatively spliced short (CRMP4a) and long (CRMP4b) isoforms are known to be involved in many biological processes [73]. In particular, CRMP4a suppresses RhoA activity, leading to reduced cytoskeletal reorganization and cell motility in prostate cancer [38]. However, further studies are needed to clarify the molecular mechanism of CRMP4 in PanIN development.

In conclusion, the incidence of high-grade PanIN was low in the CRMP4-KO mouse model of pancreatic cancer. The expression of CRMP4 in the stroma cells correlated with the progression of PanIN lesions. These findings suggest that CRMP4 inhibition may serve as a therapeutic strategy to prevent PanIN development and PDAC.

Acknowledgements

We thank Dr. Hideki Taniguchi for providing *LSL-KRAS*^{G12D} mice. We thank Ms. Harumi Sakurada and Ms. Takako Okada for their excellent technical assistance. We thank Drs. Haruko Nakamura, Yuko Kawamoto-Kondo, Aoi Takahashi-Jitsuki, Hiroko Makihara, Motokazu Koga, and Tatsuo Hashimoto for technical advice. We would like to thank Editage (www.editage.com) for English language editing. This work was supported by Grants-in-Aid from the Japanese Ministry of Education, Culture, Sports, Science, and Technology for Fundamental Research (1426462070 to I.E. and 17K10707 to Y.Y.) and Creation of Innovation Centers for Advanced Interdisciplinary Research Areas Program in the Project for Developing Innovation Systems from the MEXT (to Y.G). This work was also supported by grants from the Takei Foundation, Eli Lilly and Company, and Sanofi in Japan.

Conflict of Interest

None.

References

[1] Hidalgo M (2010). Pancreatic cancer. *New Engl J Med* **362**(17), 1605–1617.
[2] Bray F, Ferlay J, Soerjomataram I, Siegel RL, Torre LA, and Jemal A (2018). Global cancer statistics 2018: GLOBOCAN estimates of incidence and mortality worldwide for 36 cancers in 185 countries. *CA Cancer J Clin* **68**(6), 394–424.
[3] Hruban RH, Adsay NV, Albores-Saavedra J, Compton C, Garrett ES, Goodman SN, Kern SE, Klimstra DS, Klöppel G, and Longnecker DS, et al (2001). Pancreatic intraepithelial neoplasia a new nomenclature and classification system for pancreatic duct lesions. *Am J Surg Pathol* **5**(**25**), 579–586.
[4] Hruban RH and Fukushima N (2007). Pancreatic adenocarcinoma: update on the surgical pathology of carcinomas of ductal origin and PanINs. *Mod Pathol* **20**(Suppl 1), S61–S70.
[5] Guerra C and Barbacid M (2013). Genetically engineered mouse models of pancreatic adenocarcinoma. *Mol Oncol* **7**(2), 232–247.
[6] Wilentz RE, Geradts J, Maynard R, Offerhaus GJ, Kang M, Goggins M, Yeo CJ, Kern SE, and Hruban RH (1998). Inactivation of the p16 (INK4A) tumor-suppressor gene in pancreatic duct lesions: loss of intranuclear expression. *Cancer Res* **58**(20), 4740–4744.
[7] Hingorani SR, Wang L, Multani AS, Combs C, Deramaudt TB, Hruban RH, Rustgi AK, Chang S, and Tuveson DA (2005). Trp53R172H and KrasG12D cooperate to promote chromosomal instability and widely metastatic pancreatic ductal adenocarcinoma in mice. *Cancer Cell* **7**(5), 469–483.
[8] Bardeesy N, Cheng KH, Berger JH, Chu GC, Pahler J, Olson P, Hezel AF, Horner J, Lauwers GY, and Hanahan D, et al (2006). Smad4 is dispensable for normal pancreas development yet critical in progression and tumor biology of pancreas cancer. *Genes Dev* **20**(22), 3130–3146.
[9] Hansel DE, Kern SE, and Hruban RH (2003). Molecular pathogenesis of pancreatic cancer. *Annu Rev Genomics Hum Genet* **4**, 237–256.
[10] Hingorani SR, Petricoin EF, Maitra A, Rajapakse V, King C, Jacobetz MA, Ross S, Conrads TP, Veenstra TD, and Hitt BA, et al (2003). Preinvasive and invasive ductal pancreatic cancer and its early detection in the mouse. *Cancer Cell* **4**(6), 437–450.
[11] Aguirre AJ, Bardeesy N, Sinha M, Lopez L, Tuveson DA, Horner J, Redston MS, and DePinho RA (2003). Activated Kras and Ink4a/Arf deficiency cooperate to produce metastatic pancreatic ductal adenocarcinoma. *Genes Dev* **17**(24), 3112–3126.
[12] Perez-Mancera PA, Guerra C, Barbacid M, and Tuveson DA (2012). What we have learned about pancreatic cancer from mouse models. *Gastroenterology* **142**(5), 1079–1092.
[13] Gao M, Yeh PY, Lu YS, Chang WC, Kuo ML, and Cheng AL (2008). NF-kappaB p50 promotes tumor cell invasion through negative regulation of invasion suppressor gene CRMP-1 in human lung adenocarcinoma cells. *Biochem Biophys Res Commun* **376**(2), 283–287.
[14] Gao X, Pang J, Li LY, Liu WP, Di JM, Sun QP, Fang YQ, Liu XP, Pu XY, and He D, et al (2010). Expression profiling identifies new function of collapsin response mediator protein 4 as a metastasis-suppressor in prostate cancer. *Oncogene* **29**(32), 4555–4566.
[15] Mukherjee J, DeSouza LV, Micallef J, Karim Z, Croul S, Siu KW, and Guha A (2009). Loss of collapsin response mediator Protein1, as detected by iTRAQ analysis, promotes invasion of human gliomas expressing mutant EGFRvIII. *Cancer Res* **69**(22), 8545–8554.
[16] Pan SH, Chao YC, Chen HY, Hung PF, Lin PY, Lin CW, Chang YL, Wu CT, Lee YC, and Yang SC, et al (2010). Long form collapsin response mediator protein-1 (LCRMP-1) expression is associated with clinical outcome and lymph node metastasis in non–small cell lung cancer patients. *Lung Cancer* **67**(1), 93–100.
[17] Shih JY, Lee YC, Yang SC, Hong TM, Huang CY, and Yang PC (2003). Collapsin response mediator protein-1: a novel invasion-suppressor gene. *Clin Exp Metastasis* **20**(1), 69–76.
[18] Shih JY, Yang SC, Hong TM, Yuan A, Chen JJ, Yu CJ, Chang YL, Lee YC, Peck K, and Wu CW, et al (2001). Collapsin response mediator protein-1 and the invasion and metastasis of cancer cells. *J Natl Cancer Inst* **93**(18), 1392–1400.
[19] Steeg PS (2001). Collapsin response mediator protein-1: a lung cancer invasion suppressor gene with nerve. *J Natl Cancer Inst* **93**(18), 1364–1365.
[20] Wu CC, Chen HC, Chen SJ, Liu HP, Hsieh YY, Yu CJ, Tang R, Hsieh LL, Yu JS, and Chang YS (2008). Identification of collapsin response mediator protein-2 as a potential marker of colorectal carcinoma by comparative analysis of cancer cell secretomes. *Proteomics* **8**(2), 316–332.
[21] Tan F, Thiele CJ, and Li Z (2014). Collapsin response mediator proteins: potential diagnostic and prognostic biomarkers in cancers (Review). *Oncol Lett* **7**(5), 1333–1340.
[22] Goshima Y, Nakamura F, Strittmatter P, and Strittmatter SM (1995). Collapsin-induced growth cone collapse mediated by an intracellular protein related to UNC-33. *Nature* **376**(6540), 509–514.
[23] Arimura N, Inagaki N, Chihara K, Ménager C, Nakamura N, Amano M, Iwamatsu A, Goshima Y, and Kaibuchi K (2000). Phosphorylation of collapsin response mediator protein-2 by Rho-kinase. Evidence for two separate signaling pathways for growth cone collapse. *J Biol Chem* **275**(31), 23973–23980.
[24] Wang LH and Strittmatter SM (1997). Brain CRMP forms heterotetramers similar to liver dihydropyrimidinase. *J Neurochem* **69**(6), 2261–2269.
[25] Arimura N, Ménager C, Kawano Y, Yoshimura T, Kawabata S, Hattori A, Fukata Y, Amano M, Goshima Y, and Inagaki M, et al (2005). Phosphorylation by Rho kinase regulates CRMP-2 activity in growth cones. *Mol Cell Biol* **25**(22), 9973–9984.
[26] Fukata Y, Itoh TJ, Kimura T, Ménager C, Nishimura T, Shiromizu T, Watanabe H, Inagaki N, Iwamatsu A, and Hotani H, et al (2002). CRMP-2 binds to tubulin heterodimers to promote microtubule assembly. *Nat Cell Biol* **4**(8), 583–591.
[27] Rosslenbroich V, Dai L, Baader SL, Noegel AA, Gieselmann V, and Kappler J (2005). Collapsin response mediator protein-4 regulates F-actin bundling. *Exp Cell Res* **310**(2), 434–444.
[28] Khazaei MR, Girouard MP, Alchini R, Ong Tone S, Shimada T, Bechstedt S, Cowan M, Guillet D, Wiseman PW, and Brouhard G, et al (2014). Collapsin response mediator protein 4 regulates growth cone dynamics through the actin and microtubule cytoskeleton. *J Biol Chem* **289**(43), 30133–30143.
[29] Cole AR, Causeret F, Yadirgi G, Hastie CJ, McLauchlan H, McManus EJ, Hernández F, Eickholt BJ, Nikolic M, and Sutherland C (2006). Distinct priming kinases contribute to differential regulation of collapsin response mediator proteins by glycogen synthase kinase-3 in vivo. *J Biol Chem* **281**(24), 16591–16598.

[30] Sasaki Y, Cheng C, Uchida Y, Nakajima O, Ohshima T, Yagi T, Taniguchi M, Nakayama T, Kishida R, and Kudo Y, et al (2002). Fyn and Cdk5 mediate semaphorin-3A signaling, which is involved in regulation of dendrite orientation in cerebral cortex. *Neuron* **35**(5), 907–920.

[31] Uchida Y, Ohshima T, Sasaki Y, Suzuki H, Yanai S, Yamashita N, Nakamura F, Takei K, Ihara Y, and Mikoshiba K, et al (2005). Semaphorin3A signalling is mediated via sequential Cdk5 and GSK3beta phosphorylation of CRMP2: implication of common phosphorylating mechanism underlying axon guidance and Alzheimer's disease. *Genes Cells* **10**(2), 165–179.

[32] Brown M, Jacobs T, Eickholt B, Ferrari G, Teo M, Monfries C, Qi RZ, Leung T, Lim L, and Hall C (2004). Alpha2-chimaerin, cyclin-dependent Kinase 5/p35, and its target collapsin response mediator protein-2 are essential components in semaphorin 3A–induced growth-cone collapse. *J Neurosci* **24**(41), 8994–9004.

[33] Yamashita N, Morita A, Uchida Y, Nakamura F, Usui H, Ohshima T, Taniguchi M, Honnorat J, Thomasset N, and Takei K, et al (2007). Regulation of spine development by semaphorin3A through cyclin-dependent kinase 5 phosphorylation of collapsin response mediator protein 1. *J Neurosci* **46**(**27**), 12546–12554.

[34] Uchida Y, Ohshima T, Yamashita N, Ogawara M, Sasaki Y, Nakamura F, and Goshima Y (2009). Semaphorin3A signaling mediated by Fyn-dependent tyrosine phosphorylation of collapsin response mediator protein 2 at tyrosine 32. *J Biol Chem* **40**(**284**), 27393–27401.

[35] Nakamura F, Kumeta K, Hida T, Isono T, Nakayama Y, Kuramata-Matsuoka E, Yamashita N, Uchida Y, Ogura K, and Gengyo-Ando K, et al (2014). Amino- and carboxyl-terminal domains of Filamin-A interact with CRMP1 to mediate Sema3A signalling. *Nat Commun* **5**, 5325.

[36] Manivannan J, Tay SS, Ling EA, and Dheen ST (2013). Dihydropyrimidinase-like 3 regulates the inflammatory response of activated microglia. *Neuroscience* **253**, 40–54.

[37] Tonouchi A, Nagai J, Togashi K, Goshima Y, and Ohshima T (2016). Loss of collapsin response mediator protein 4 suppresses dopaminergic neuron death in an 1-methyl-4-phenyl-1,2,3,6-tetrahydropyridine-induced mouse model of Parkinson's disease. *J Neurochem* **137**(5), 795–805.

[38] Li C, Xu H, Xiao L, Zhu H, Zhang G, Wei W, Li K, Cao X, Shen D, and Holzbeierlein J, et al (2018). CRMP4a suppresses cell motility by sequestering RhoA activity in prostate cancer cells. *Cancer Biol Ther* **19**(12), 1193–1203.

[39] Kanda M, Nomoto S, Oya H, Shimizu D, Takami H, Hibino S, Hashimoto R, Kobayashi D, Tanaka C, and Yamada S, et al (2014). Dihydropyrimidinase-like 3 facilitates malignant behavior of gastric cancer. *J Exp Clin Cancer Res* **33**, 66.

[40] Guo H and Xia B (2016). Collapsin response mediator protein 4 isoforms (CRMP4a and CRMP4b) have opposite effects on cell proliferation, migration, and invasion in gastric cancer. *BMC Cancer* **16**, 565.

[41] Chen SL, Cai SR, Zhang XH, Li WF, Zhai ET, Peng JJ, Wu H, Chen CQ, Ma JP, and Wang Z, et al (2016). Targeting CRMP-4 by lentivirus-mediated RNA interference inhibits SW480 cell proliferation and colorectal cancer growth. *Exp Ther Med* **12**(4), 2003–2008.

[42] Oya H, Kanda M, Sugimoto H, Shimizu D, Takami H, Hibino S, Hashimoto R, Okamura Y, Yamada S, and Fujii T, et al (2015). Dihydropyrimidinase-like 3 is a putative hepatocellular carcinoma tumor suppressor. *J Gastroenterol* **50**(5), 590–600.

[43] Hiroshima Y, Nakamura F, Miyamoto H, Mori R, Taniguchi K, Matsuyama R, Akiyama H, Tanaka K, Ichikawa Y, and Kato S, et al (2013). Collapsin response mediator protein 4 expression is associated with liver metastasis and poor survival in pancreatic cancer. *Ann Surg Oncol* **20 Suppl 3**, S369–S378.

[44] Kawahara T, Hotta N, Ozawa Y, Kato S, Kano K, Yokoyama Y, Nagino M, Takahashi T, and Yanagisawa K (2013). Quantitative proteomic profiling identifies DPYSL3 as pancreatic ductal adenocarcinoma-associated molecule that regulates cell adhesion and migration by stabilization of focal adhesion complex. *PLoS One* **8**(12)e79654.

[45] Wu Y, Wei J, Ming Y, Chen Z, Yu J, Mao R, Chen H, Zhou G, and Fan Y (2018). Orchestrating a biomarker panel with lncRNAs and mRNAs for predicting survival in pancreatic ductal adenocarcinoma. *J Cell Biochem* **119**(9), 7696–7706.

[46] Sato S, Nakamura F, Hiroshima Y, Nagashima Y, Kato I, Yamashita N, Goshima Y, and Endo I (2016). Caerulein-induced pancreatitis augments the expression and phosphorylation of collapsin response mediator protein 4. *J Hepatobiliary Pancreat Sci* **23**(7), 422–431.

[47] Raimondi S, Lowenfels AB, Morselli-Labate AM, Maisonneuve P, and Pezzilli R (2010). Pancreatic cancer in chronic pancreatitis; aetiology, incidence, and early detection. *Best Pract Res Clin Gastroenterol* **24**(3), 349–358.

[48] Kolodecik T, Shugrue C, Ashat M, and Thrower EC (2013). Risk factors for pancreatic cancer: underlying mechanisms and potential targets. *Front Physiol* **4**, 415.

[49] Jackson EL, Willis N, Mercer K, Bronson RT, Crowley D, Montoya R, Jacks T, and Tuveson DA (2001). Analysis of lung tumor initiation and progression using conditional expression of oncogenic K-ras. *Genes Dev* **15**(24), 3243–3248.

[50] Niisato E, Nagai J, Yamashita N, Abe T, Kiyonari H, Goshima Y, and Ohshima T (2012). CRMP4 suppresses apical dendrite bifurcation of CA1 pyramidal neurons in the mouse hippocampus. *Dev Neurobiol* **72**(11), 1447–1457.

[51] Nagai J, Kitamura Y, Owada K, Yamashita N, Takei K, Goshima Y, and Ohshima T (2015). Crmp4 deletion promotes recovery from spinal cord injury by neuroprotection and limited scar formation. *Sci Rep* **5**, 8269.

[52] Riken center for development biology. (n.d.), Laboratories: animal resource development unit and genetic engineering team Riken CLST, Retrieved September 17, 2019, from http://www.cdb.riken.jp/arg/mutant%20mice%20list.html.

[53] Carrière C, Young AL, Gunn JR, Longnecker DS, and Korc M (2009). Acute pancreatitis markedly accelerates pancreatic cancer progression in mice expressing oncogenic Kras. *Biochem Biophys Res Commun* **382**(3), 561–565.

[54] Willemer S, Elsässer HP, and Adler G (1992). Hormone-induced pancreatitis. *Eur Surg Res* **24** (Suppl 1), 29–39.

[55] Hruban RH, Adsay NV, Albores-Saavedra J, Anver MR, Biankin AV, Boivin GP, Furth EE, Furukawa T, Klein A, and Klimstra DS, et al (2006). Pathology of genetically engineered mouse models of pancreatic exocrine cancer: consensus report and recommendations. *Cancer Res* **66**(1), 95–106.

[56] Cornish TC and Hruban RH (2011). Pancreatic intraepithelial neoplasia. *Surg Pathol Clin* **4**(2), 523–535.

[57] Guerra C, Collado M, Navas C, Schuhmacher AJ, Hernández-Porras I, Cañamero M, Rodriguez-Justo M, Serrano M, and Barbacid M (2011). Pancreatitis-induced inflammation contributes to pancreatic cancer by inhibiting oncogene-induced senescence. *Cancer Cell* **19**(6), 728–739.

[58] Clark CE, Hingorani SR, Mick R, Combs C, Tuveson DA, and Vonderheide RH (2007). Dynamics of the immune reaction to pancreatic cancer from inception to invasion. *Cancer Res* **67**(19), 9518–9527.

[59] Pandol S, Edderkaoui M, Gukovsky I, Lugea A, and Gukovskaya A (2009). Desmoplasia of pancreatic ductal adenocarcinoma. *Clin Gastroenterol Hepatol* **7**(11 Suppl), S44–S47.

[60] Apte MV, Wilson JS, Lugea A, and Pandol SJ (2013). A starring role for stellate cells in the pancreatic cancer microenvironment. *Gastroenterology* **144**(6), 1210–1219.

[61] Apte MV, Haber PS, Applegate TL, Norton ID, McCaughan GW, Korsten MA, Pirola RC, and Wilson JS (1998). Periacinar stellate shaped cells in rat pancreas: identification, isolation, and culture. *Gut* **43**(1), 128–133.

[62] Wilson JS, Pirola RC, and Apte MV (2014). Stars and stripes in pancreatic cancer: role of stellate cells and stroma in cancer progression. *Front Physiol* **5**, 52.

[63] Apte MV, Park S, Phillips PA, Santucci N, Goldstein D, Kumar RK, Ramm GA, Buchler M, Friess H, and McCarroll JA, et al (2004). Desmoplastic reaction in pancreatic cancer: role of pancreatic stellate cells. *Pancreas* **29**(3), 179–187.

[64] Masamune A, Watanabe T, Kikuta K, and Shimosegawa T (2009). Roles of pancreatic stellate cells in pancreatic inflammation and fibrosis. *Clin Gastroenterol Hepatol* **7**(11 Suppl), S48–S54.

[65] Jakkampudi A, Jangala R, Reddy BR, Mitnala S, Nageshwar Reddy D, and Talukdar R (2016). NF-kappaB in acute pancreatitis: mechanisms and therapeutic potential. *Pancreatology* **16**(4), 477–488.

[66] Pandol S, Gukovskaya A, Edderkaoui M, Dawson D, Eibl G, and Lugea A (2012). Epidemiology, risk factors, and the promotion of pancreatic cancer: role of the stellate cell. *J Gastroenterol Hepatol* **27** (2Suppl), 127–134.

[67] Omary MB, Lugea A, Lowe AW, and Pandol SJ (2007). The pancreatic stellate cell: a star on the rise in pancreatic diseases. *J Clin Invest* **117**(1), 50–59.

[68] Liou GY, Döppler H, Necela B, Edenfield B, Zhang L, Dawson DW, and Storz P (2015). Mutant KRAS-induced expression of ICAM-1 in pancreatic acinar cells causes attraction of macrophages to expedite the formation of precancerous lesions. *Cancer Discov* **5**(1), 52–63.

[69] Hruban RH, Maitra A, and Goggins M (2008). Update on pancreatic intraepithelial neoplasia. *Int J Clin Exp Pathol* **1**(4), 306–316.

[70] Bi Y, Page SL, and Williams JA (2005). Rho and Rac promote acinar morphological changes, actin reorganization, and amylase secretion. *Am J Physiol Gastrointest Liver Physiol* **289**(3), G561–G570.

[71] Heid I, Lubeseder-Martellato C, Sipos B, Mazur PK, Lesina M, Schmid RM, and Siveke JT (2011). Early requirement of Rac1 in a mouse model of pancreatic cancer. *Gastroenterology* **2**(**141**), 719–730 730.e1–7.

[72] Tan M, Cha C, Ye Y, Zhang J, Li S, Wu F, Gong S, and Guo G (2015). CRMP4 and CRMP2 interact to coordinate cytoskeleton dynamics, regulating growth cone development and axon elongation. *Neural Plast* **2015**, 947423.

[73] Quinn CC, Chen E, Kinjo TG, Kelly G, Bell AW, Elliott RC, McPherson PS, and Hockfield S (2003). TUC-4b, a novel TUC family variant, regulates neurite outgrowth and associates with vesicles in the growth cone. *J Neurosci* **23**(7), 2815–2823.